

Layer-by-Layer Structured Gelatin Nanofiber Membranes with Photoinduced Antibacterial Functions

Ang Lu,¹ Zhaocheng Ma,² Jingyuan Zhuo,¹ Gang Sun,¹ Guodong Zhang³

¹Fiber and Polymer Science, University of California, Davis, California 95616

²College of Horticulture and Forestry Sciences, Huazhong Agricultural University, Wuhan 430070, China

³Department of Food Science, University of Wisconsin—Madison, Wisconsin, 53706-1565

All authors contributed equally to this work.

Correspondence to: G. Sun (E-mail: gysun@ucdavis.edu)

ABSTRACT: Gelatin (GE) nanofiber suspensions prepared by the extrusion of an immiscible polymer solution blend were cast into nanofibrous membranes. An organic chemical capable of generating radicals under photoexposure, anthraquinone-2,6-disulfonic acid (AQS), was assembled layer by layer (LBL) onto the gelatin nanofiber membranes. The composite gelatin nanofibrous membranes assembled with AQS demonstrated excellent photoinduced antibacterial properties by killing bacteria. Scanning electron microscopy images demonstrated that the composite nanofibrous membranes maintained a well-defined nanofiber morphology and large specific surface area after LBL assembly. Moreover, the nanofiber morphology and nanofibrous structure of the composite nanofibrous membranes were completely reserved after photoexposure. An analysis of the cell indicated that the composite gelatin nanofibrous membranes assembled with AQS exhibited the same biocompatibility as the original gelatin nanofibers. These results demonstrate that AQS LBL-assembled gelatin nanofibrous membranes could be a potential candidate for wound dressing applications. © 2012 Wiley Periodicals, Inc. *J. Appl. Polym. Sci.* 000: 000–000, 2012

KEYWORDS: nanofiber, extrusion, gelatin, layer-by-layer

Received 18 April 2012; accepted 1 June 2012; published online

DOI: 10.1002/app.38131

INTRODUCTION

When their diameters decrease from microscale to nanoscale, polymer fiber materials exhibit amazing properties and functions, for example, an enormous surface area to volume ratio, flexibility in material surface functionalities, and remarkable mechanical properties, compared with other known new materials.¹ These outstanding properties and functions make polymer nanofiber materials an optimal candidate for many different and important applications in all kinds of field, including filtration,² sensors,^{3–5} photonics,⁶ and medical and pharmaceutical fields.^{7–10}

In our laboratory, a novel approach for nanofiber fabrication was established, that is, the extrusion of an immiscible polymer solution blend. Moreover, gelatin (GE) nanofiber suspensions were successfully fabricated that demonstrated a remarkable promotion to cell adhesion and are applicable to the tissue engineering field.¹¹ As a natural polymer derived from collagen, gelatin contains many functional groups.^{12–14} It is a biodegradable polymer with a lot of attractive properties, including excellent biocompatibility, plasticity, nonantigenicity, and adhesive-

ness,¹⁵ and has been blended with other materials to promote cell adhesion, migration, differentiation, and proliferation.^{16–19} Therefore, it has widespread applications in medical devices as wound dressings, plasma expanders, adhesives, absorbent pads for surgical use, and biopharmaceutical materials for drug-controlled release.^{20–24}

On the other hand, photocatalytic substances capable of generating highly reactive superoxide and hydroxyl radicals have attracted lots of attention for nanofiber functionalization because the generated reactive oxygen species (ROS) are able to decompose hazardous chemicals and inactivate bacteria under light.^{25–27} A combination of gelatin nanofibers with photocatalytic substances would make these materials a potential candidate for wound dressings.

In this study, we examined a novel photoinduced antibacterial layer-by-layer (LBL)-structured gelatin nanofiber membrane. A negatively charged photocatalytic compound, anthraquinone-2,6-disulfonic acid (AQS), was selected and adsorbed onto the surfaces of gelatin nanofibers in the form of an ultrathin conformational coating with LBL deposition with positively charged

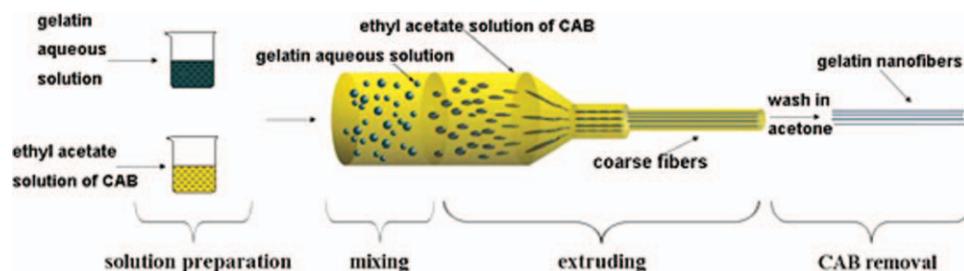


Figure 1. Schematic diagram of gelatin nanofiber fabrication via the extrusion of an immiscible polymer solution blend of a gelatin aqueous solution and an ethyl acetate solution of cellulose acetate butyrate (CAB).¹¹ [Color figure can be viewed in the online issue, which is available at wileyonlinelibrary.com.]

gelatin molecules. The morphology of the nanofibers, antibacterial efficiency against *Escherichia coli*, and cytotoxicity were investigated.

EXPERIMENTAL

Materials

Cellulose acetate butyrate (CAB; 13.5 wt % acetyl content and 37 wt % butyryl content) and ethyl acetate (anhydrous) were purchased from the Aldrich Chemical Co. (St. Louis, MO). AQS disodium salt was purchased from Acros Chemical Co. (Pittsburgh, PA). Gelatin was purchased from Sinopharm Chemical Reagent Co., Ltd. (Shanghai, China). Hydrogen peroxide (H_2O_2) test strips were purchased from Indigo Instruments (Waterloo, Ontario, Canada). All materials were used without further purification.

Fabrication of the gelatin nanofiber membranes

The gelatin nanofibers were fabricated via the extrusion of an immiscible polymer solution blend of a gelatin aqueous solution and an ethyl acetate solution of CAB, as schematically demonstrated in Figure 1.¹¹ CAB was dissolved in ethyl acetate at room temperature, and gelatin was dissolved in distilled water at 60°C. We prepared the CAB/gelatin immiscible solution blend by feeding the solutions into a mixer with a stirring speed of 300 rpm; then, the gelatin solution was dispersed as small droplets into the CAB solution matrix. Next, the immiscible polymer solution blend was extruded through a capillary rheometer LCR 8052 (Kayness, PA, USA) with a capillary round die with a length-to-diameter ratio of 30 and an entrance angle of 120°, and the composite coarse fibers were drawn and collected in hot air generated by two electric blowers. All of the CAB/gelatin coarse fibers were dried for 24 h at 120°C and

stored in desiccators until subsequent use. The composite coarse fibers were transferred into polypropylene centrifuge tubes containing acetone, and the tubes were shaken at room temperature for 24 h to remove CAB from the blends. The gelatin nanofibers were obtained in dispersion form (the gelatin nanofibers formed a milky white suspension in acetone without any further mechanical treatment). We then fabricated the gelatin nanofibrous membranes by casting and drying the suspension *in vacuo*; then, the gelatin nanofibrous membranes were crosslinked with glutaraldehyde in a mixed solvent of deionized water and ethanol. The crosslinked gelatin nanofibrous membranes were then used for the LBL procedure.

LBL self-assembly of the photocatalytic compound

The photoactive compound, AQS, was assembled on the gelatin nanofibrous membranes by alternate adsorptions of positively charged gelatin and negatively charged AQS according to the following details. A schematic diagram is shown in Figure 2. Gelatin was dissolved in deionized water to form an aqueous solution with a concentration of 2 mg/mL, and the pH value was controlled at 3.0. The concentration of the AQS aqueous solution was also 2 mg/mL, and the pH value was controlled at 3.0. The aforementioned crosslinked gelatin nanofibrous membranes were immersed in the gelatin solution for 20 min. The membranes were then rinsed twice with deionized water for 2 min each. The rinsed membranes were subsequently immersed in AQS solutions for another 20 min; this was followed by the same rinsing steps to obtain the one-bilayer assembly-structured film on gelatin nanofiber membranes. The electrostatic adsorption and rinsing steps were repeated two more times to make the three-bilayer assembly-structured gelatin/AQS nanofibrous membranes.

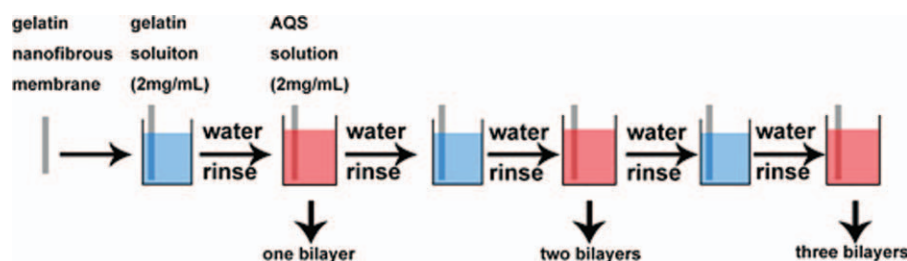


Figure 2. Schematic diagram of the fabrication of the layer-by-layer (LBL) structured gelatin nanofiber membranes. AQS: anthraquinone-2,6-disulfonate, disodium. [Color figure can be viewed in the online issue, which is available at wileyonlinelibrary.com.]

Characterization

The gelatin nanofibers membranes and different bilayer gelatin/AQS nanofibrous membranes before and after UVA (365 nm) exposure were observed with a Philips XL30 scanning electron microscope (FEI, Hillsboro, OR, USA). One hundred fibers were used to calculate the number-average diameter (D_N) and distribution of nanofiber diameters. D_N was calculated as follows:

$$D_N = \frac{\sum N_i D_i}{\sum N_i} \quad (1)$$

where N_i is the number of nanofibers with a diameter of D_i .

Detection of H_2O_2

Several pieces of gelatin/AQS nanofibrous membranes were exposed to UVA for 1 h. After that, one droplet of deionized water was dropped onto the membranes to dissolve the generated H_2O_2 . Sixty seconds later, H_2O_2 test strips were used to test the generation of H_2O_2 by through contact with the water.

Antibacterial testing

The antibacterial properties of the gelatin/AQS nanofibrous membranes were examined against *E. coli* (K-12, a Gram-negative bacterium), according to a modified AATCC 100 test method. The same gelatin nanofiber membrane without any treatment was used as a control. Four 2.5×2.5 cm² swatches of the control or the three-bilayer gelatin/AQS nanofibrous membranes were placed in two separate sterilized Petri dishes. An aqueous suspension (1.0 mL) containing *E. coli* was evenly dropped onto the surfaces of the samples, and then, both were illuminated under UVA irradiation or no irradiation for 1 h. Both samples were placed into separate containers containing 100 mL of sterilized distilled water. The mixture was vigorously shaken for 1 min. Then, 100 μ L of the aqueous solution was taken from the container and diluted 10^0 , 10^1 , 10^2 , and 10^3 times in sequence. Finally, 100 μ L of the solution at different stages of dilution was placed onto four equal zones of a nutrient agar plate, and the agar plate was incubated at 37°C for 18 h.

To perform a modified Kirby–Bauer type test for the gelatin nanofiber membrane and gelatin/AQS nanofibrous membrane without UVA exposure, two membrane samples were cut into equal-sized pieces, and each piece was placed on *E. coli* grown on an agar plate. After 18 h of incubation at 37°C, the zone of inhibition was measured.

Cell culture

HepG2 cells (HB-8065, ATCC, Manassas, VA) were cultured in Eagle's minimal essential medium supplemented with 10% fetal bovine serum and antibiotics in a 37°C incubator with a 5% CO₂ atmosphere. The HepG2 cells were seeded onto the UVA-exposed gelatin nanofiber membranes and three-bilayer gelatin/AQS nanofibrous membranes, respectively, in six-well plates (100,000 cells/well in 1 mL of medium); after 24 h of incubation, the cell viability was assessed by a 3-(4,5-dimethylthiazol-2-yl)-2,5-diphenyltetrazolium bromide cell viability kit (ATCC) according to the manufacturer's instructions. Briefly, 0.5 mL of 3-(4,5-dimethylthiazol-2-yl)-2,5-diphenyltetrazolium bromide reagent was added directly to each well and incubated at 37°C for 2 h. Then, 1 mL of detergent reagent was added to each well and incubated in the dark at room temperature overnight.

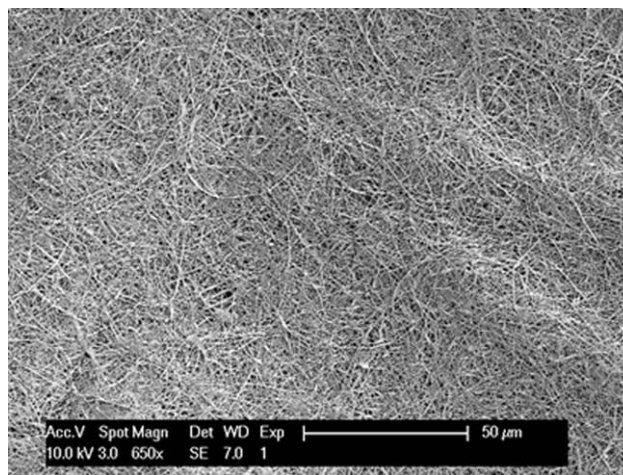


Figure 3. SEM images of the gelatin nanofibers fabricated via an extrusion approach (CAB solution/gelatin solution = 90/10).

The absorbance at 575 nm was measured by a microplate reader (Molecular Devices, Sunnyvale, CA).

RESULTS AND DISCUSSION

A gelatin (GE) aqueous solution and ethyl acetate solution of CAB were mixed to form an immiscible polymer solution blend, and the composite coarse fibers were collected after extrusion. Gelatin nanofiber suspensions were obtained after CAB removal in acetone for 24 h.¹¹ Figure 3 shows the scanning electron microscopy (SEM) image of the gelatin nanofiber membranes fabricated via the extrusion approach (CAB solution/gelatin solution = 90/10). The image shows well-defined and continuous nanofiber bundles with small diameters and a uniform diameter distribution. The diameters of the gelatin nanofibers ranged from about 50 to 500 nm, and the average diameter was about 210 nm; this was in accordance with our previous study.¹¹ The nanofiber morphology and nanofiber structure might make it a potential candidate for wound dressing.

Generally, there were two concerns associated with the functionalization of the nanofiber membranes. One was whether the introduction of the active substances to the nanofiber membranes could have led to a loss of surface area. The other one was whether the sufficient photoinduced antibacterial properties could damage the supporting nanofiber materials. Figure 4 shows the morphologies of the gelatin nanofiber membranes assembled with one, two, and three bilayers of gelatin and anthraquinone-2,6-disulfonic acid (AQS) and the morphologies of these membranes after 1 h of UVA exposure. Compared with Figure 3, there was no significant difference observed [Figure 4(a–c)]; this suggested the LBL assembly with AQS could have formed a conformal coating on the gelatin nanofibers without compromising the surface area. Moreover, the diameters of the different bilayer gelatin/AQS nanofibers did not differ much; this indicated a very thin layer of gelatin and AQS compound on the original gelatin nanofiber surface. After UVA exposure, SEM was also applied to investigate whether the sufficient

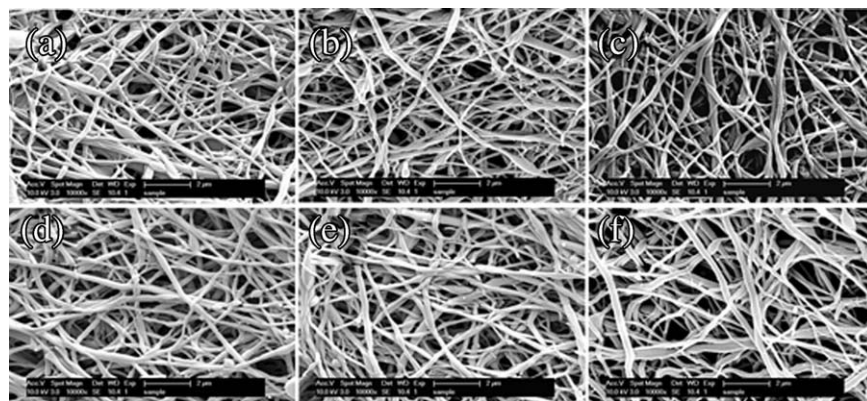


Figure 4. SEM images of AQS-assembled gelatin nanofibrous membranes with (a) one, (b) two, and (c) three bilayers and SEM images of AQS-assembled gelatin nanofibrous membranes with (d) one, (e) two, and (f) three bilayers after 1 h of UVA exposure.

photoinduced antibacterial properties could have damaged the supporting nanofibrous materials, as shown in Figure 4(d–f). Obviously, although the AQS-assembled gelatin nanofibrous membranes demonstrated excellent photoinduced antibacterial activities (see later), the surface morphology was well-maintained. The nanofiber morphology and nanofibrous structure were reserved; this indicated that the UVA exposure and ROS generation had no influence on the supporting gelatin nanofiber structure. The results suggest that the nanofibrous structure could last for a long time for the antibacterial properties and, on the other hand, could supply nutrition to the cells around the wound.

The AQS could have been excited to the singlet state under UV light irradiation and then efficiently intersystem-crossed to triplet states for diaryl ketone, which could have easily abstracted a hydrogen atom from a weak C–H bond or other hydrogen donor to form a ketyl radical.^{28–30} The reaction of ketyl radicals with oxygen could then produce active superoxide, peroxide, and hydroxyl radicals, which were capable of degrading pollutants and inactivating bacteria. In this study, H₂O₂ test strips were applied to test the generation of H₂O₂ by the gelatin/AQS

nanofibrous membranes after exposure for 1 h to UVA to verify the presence of AQS. Figure 5 shows the images of H₂O₂ testing results of one-, two-, and three-bilayer AQS-assembled gelatin nanofiber membranes after 1 h of UVA exposure. According to the results, the one-, two-, and three-bilayer gelatin/AQS nanofibrous membranes all generated H₂O₂, however, in different amounts. The blue color shown in Figure 5(a) indicates that the one-bilayer gelatin/AQS nanofibrous membranes generated about 30 ppm H₂O₂ after 1 h of UVA exposure. The three-bilayer membrane was black; this demonstrated an H₂O₂ generation of more than 100 ppm [Figure 5(c)]. The two-bilayer gelatin/AQS membrane had an H₂O₂ yield between them, as shown in Figure 5(b). The results suggest that the H₂O₂ generation was directly influenced by the AQS amount, which was dominated by the bilayer numbers of gelatin and AQS.

The antibacterial properties of the AQS by LBL assembly on the gelatin nanofiber membranes after 1 h of UVA exposure were examined against *E. coli* according to a modified AATCC 100 method, and the results are shown in Figure 6. The membranes without and with the assembly of AQS compounds were inoculated with *E. coli* bacterial solutions with concentrations of 10⁵–10⁶ CFU/mL and then irradiated under UVA light (365 nm) for

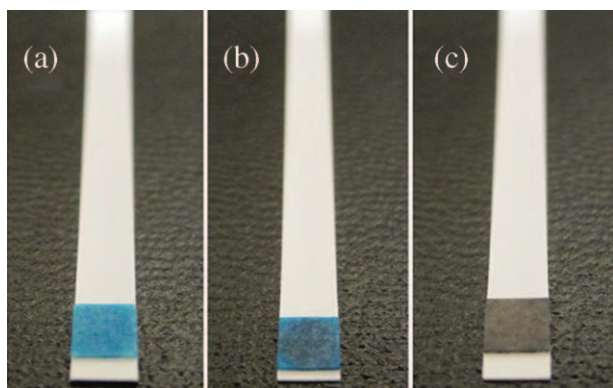


Figure 5. Images of H₂O₂ test strips after the detection of the H₂O₂ generation of (a) one-, (b) two-, and (c) three-bilayer AQS-assembled gelatin nanofibrous membranes after 1 h of UVA exposure. [Color figure can be viewed in the online issue, which is available at wileyonlinelibrary.com.]

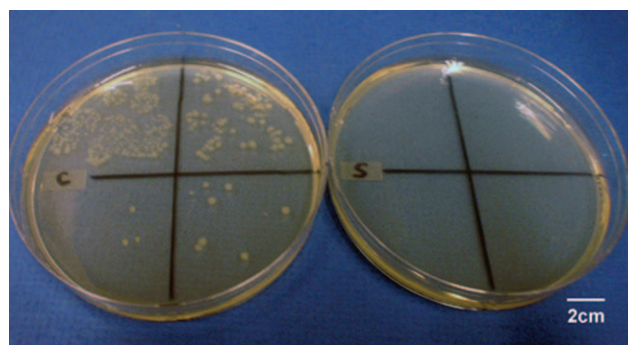


Figure 6. Antibacterial test of the three-bilayer AQS-assembled gelatin nanofibrous membranes after UVA exposure for 1 h. (S = sample, and C = control). [Color figure can be viewed in the online issue, which is available at wileyonlinelibrary.com.]

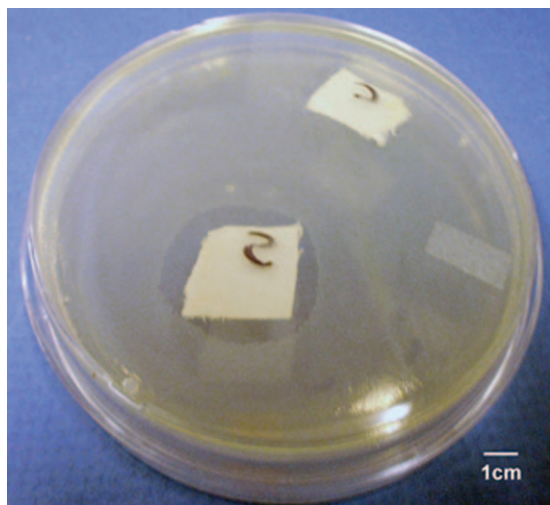


Figure 7. Antibacterial test of the three-bilayer AQS-assembled gelatin nanofibrous membrane without UVA exposure. (S = sample, C = control). [Color figure can be viewed in the online issue, which is available at wileyonlinelibrary.com.]

1 h. No viable colony of the bacteria was found on the agar plate for the gelatin nanofibrous membranes assembled with AQS compounds, whereas proliferated colonies of *E. coli* were observed for the gelatin nanofiber membranes without AQS assembly. The reduction rate of the *E. coli* bacteria indicated that the AQS-assembled gelatin nanofiber membranes exhibited excellent photoinduced antibacterial properties.

Figure 7 shows the antibacterial test results of the gelatin nanofiber membrane and three-bilayer AQS-assembled gelatin nanofibrous membrane without UVA exposure. A clear zone of inhibition around the gelatin/AQS nanofibrous membrane after 18 h of incubation was observed, in comparison with the gelatin nanofiber control group, which did not show any inhibitory effect on the growth of *E. coli*. The results suggest that the small

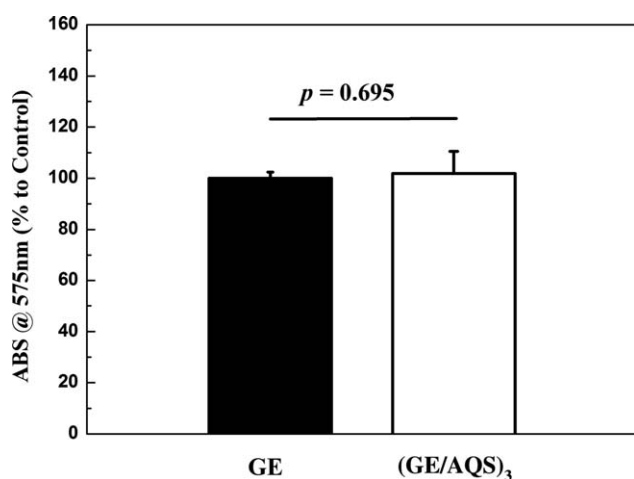


Figure 8. Variable of HepG2 cells seeded on gelatin nanofiber membranes (control) and three-bilayer gelatin/AQS nanofibrous membranes after 24 h of culturing. ABS: absorbance; GE: gelatin nanofibrous membrane; GE/AQS: three bilayer gelatin/AQS nanofibrous membranes.

amount of UV existing in the environment was still able to excite AQS in the nanofibrous membranes. However, the small inhibition zone suggested that the excitement was weak and showed weaker antibacterial properties compared to the one under intensive UVA exposure.

These results indicate that the AQS-assembled gelatin nanofibrous membranes effectively inhibited bacterial growth as much as biocides. The significant reduction of bacterial growth under UVA exposure decreased the possibility of biofilm development. The gelatin/AQS nanofibrous membranes were capable of different conditions: a burst release under UVA exposure is highly desirable for most infection cases (Figure 6), and many studies have proven its efficacy.^{31,32} Furthermore, the small amount ROS generation without intensive UVA exposure is suitable for the curing of wounds (Figure 7), in which case a burst release of antibacterial agents is not necessary.

An ideal wound dressing should not release toxic products or produce adverse reactions; this can be evaluated through *in vitro* cytotoxicity tests. Figure 8 shows the variability of HepG2 cells seeded on gelatin nanofiber membranes (control) and three-bilayer gelatin/AQS nanofibrous membranes after 24 h of culture, before which both the control and gelatin/AQS nanofibrous membranes were exposed to UVA for 1 h. No statistically significant differences were observed in the cell activity after 24 h on the three-bilayer gelatin/AQS nanofibrous membranes in comparison with the control. The obtained results clearly suggest that the gelatin/AQS nanofibrous membranes were nontoxic to cells and are good candidates for wound dressing applications.

CONCLUSIONS

Photoactive AQS compounds were assembled LBL onto the surfaces of gelatin nanofiber membranes. SEM images demonstrated that the composite nanofibrous membranes maintained a well-defined nanofiber morphology and a large specific surface area after LBL assembly. Moreover, the nanofiber morphology and nanofibrous structure of the composite membranes were completely reserved after photoexposure. The radical amount generated by UV exposure was directly influenced by the AQS amount of the gelatin/AQS membranes, which was dominated by the bilayer numbers. The composite gelatin nanofibrous membranes assembled with AQS demonstrated excellent photoinduced antibacterial properties, and cell tests indicated that the composite gelatin nanofibrous membranes assembled with AQS had the same biocompatibility as the original gelatin nanofibers. These results demonstrate that AQS LBL-assembled gelatin nanofibrous membranes could be a potential candidate for wound dressing applications.

ACKNOWLEDGMENTS

The authors thank Jie Zhang for her contribution to this work. This study was financially supported by Defense Threat Reduction Agency (grant number HDTRA1-08-1-0005).

REFERENCES

- Huang, Z. M.; Zhang, Y. Z.; Kotaki, M.; Ramakrishna, S. *Compos. Sci. Technol.* **2003**, *63*, 2223.

2. Gopal, R.; Kaur, S.; Ma, Z. W.; Chan, C.; Ramakrishna, S.; Matsuura, T. *J. Membr. Sci.* **2006**, *281*, 581.
3. Li, Z. Y.; Zhang, H. N.; Zheng, W.; Wang, W.; Huang, H. M.; Wang, C.; MacDiarmid, A. G.; Wei, Y. *J. Am. Chem. Soc.* **2008**, *130*, 5036.
4. Liu, H. Q.; Kameoka, J.; Czaplewski, D. A.; Craighead, H. G. *Nano. Lett.* **2004**, *4*, 671.
5. Wu, H.; Sun, Y.; Lin, D. D.; Zhang, R.; Zhang, C.; Pan, W. *Adv. Mater.* **2009**, *21*, 227.
6. Tomczak, N.; van Hulst, N. F.; Vancso, G. J. *Macromolecules* **2005**, *38*, 7863.
7. Nagarajan, R.; Drew, C.; Mello, C. M. *J. Phys. Chem. C* **2007**, *111*, 16105.
8. Qi, H.; Hu, P.; Xu, J.; Wang, A. *Biomacromolecules* **2006**, *7*, 2327.
9. Chew, S. Y.; Wen, J.; Yim, E. K. F.; Leong, K. W. *Biomacromolecules* **2005**, *6*, 2017.
10. Wang, F.; Li, Z.; Tamama, K.; Sen, C. K.; Guan, J. *Biomacromolecules* **2009**, *10*, 2609.
11. Lu, A.; Zhu, J.; Zhang, G. D.; Sun, G. *J. Mater. Chem.* **2011**, *21*, 18674.
12. Liu, Y.; Shu, X. Z.; Gray, S. D.; Prestwich, G. D. *J. Biomed. Mater. Res. A* **2004**, *68*, 142.
13. Chang, M. C.; Ko, C. C.; Douglas, W. H. *Biomaterials* **2003**, *24*, 3087.
14. Lee, S. B.; Jeon, H. W.; Lee, Y. W.; Lee, Y. M.; Song, K. W.; Park, H.; Nam, Y. S.; Ahn, H. C. *Biomaterials* **2003**, *24*, 2503.
15. Vlierberghe, S. V.; Cnudde, V.; Dubruel, P.; Masschaele, B.; Cosijns, A.; Paepe, I. D.; Jacobs, P. J.; Hoorebeke, L. V.; Remon, J. P.; Schacht, E. *Biomacromolecules* **2007**, *8*, 331.
16. Eser Elcin A.; Elcin, Y. M.; Pappas, G. D. *Neurol. Res.* **1998**, *20*, 648.
17. Sun, J. S.; Wu, S. Y. H.; Lin, F. H. *Biomaterials* **2005**, *26*, 3953.
18. Chang, C. H.; Lin, F. H.; Lin, C. C.; Chou, C. H.; Liu, H. C. *J. Biomed. Mater. Res. B* **2004**, *71*, 313.
19. Kim, H. W.; Kim, H. E.; Salih, V. *Biomaterials* **2005**, *26*, 5221.
20. Huang, Y.; Onyeri, S.; Siewe, M.; Moshfeghian, A.; Madhally, S. V. *Biomaterials* **2005**, *26*, 7616.
21. Dubruel, P.; Unger, R.; Vlierberghe, S. V.; Cnudde, V.; Jacobs, P. J. S.; Schacht, E.; Kirkpatrick, C. J. *Biomacromolecules* **2007**, *8*, 338.
22. Fukunaka, Y.; Iwanaga, K.; Morimoto, K.; Kakemi, M.; Tabata, Y. *Controlled. Release.* **2002**, *80*, 333.
23. Changez, M.; Koul, V.; Krishna, B. *Biomaterials* **2004**, *25*, 139.
24. Balakrishnan, B.; Mohanty, M.; Umashankar, P. R.; Jayakrishnan, A. *Biomaterials* **2005**, *26*, 6335.
25. Parkin, I. P.; Palgrave, R. G. *J. Mater. Chem.* **2005**, *15*, 1689.
26. Wang, D.; Liu, N.; Xu, W. L.; Sun, G. *J. Phys. Chem. C* **2011**, *115*, 6825.
27. Liu, N.; Sun, G.; Zhu, J. *J. Mater. Chem.* **2011**, *21*, 15383.
28. Liu, N.; Sun, G. *Ind. Eng. Chem. Res.* **2011**, *50*, 5326.
29. Liu, N.; Sun, G. *Dyes. Pigments.* **2011**, *91*, 215.
30. Liu, N.; Sun, G. *Am. Chem. Soc. Appl. Mater. Interfaces.* **2011**, *3*, 1221.
31. Shukla, A.; Fleming, K. E.; Chuang, H. F.; Chau, T. M.; Loose, C. R.; Stephanopoulos, G. N.; Hammond, P. T. *Biomaterials* **2010**, *31*, 2348.
32. Stallmann, H. P.; Faber, C.; Slotema, E. T.; Lyaruu, D. M.; Lyaruu, A. L.; Bronckers, J. J.; Amerongen, A. V. N.; Wuisman, P. I. J. M. *J. Antimicrob. Chemother.* **2003**, *52*, 853.